

Microphysical approach to polarized radiative transfer: extension to the case of an external observation point

Michael I. Mishchenko

The self-consistent microphysical approach applied recently to the transfer of polarized radiation inside a volume of anisotropic discrete random medium is extended to the case of an external observation point. Specifically, it is demonstrated that the solution of the vector radiative transfer equation yields all quantities necessary to calculate the response of an external collimated detector of polarized radiation as a function of the detector orientation and position relative to the scattering volume.

OCIS codes: 030.5620, 260.2110, 260.5430, 280.1310, 290.4210, 290.5850.

1. Introduction

In a recent paper,¹ I used methods of statistical electromagnetics to give a self-consistent microphysical derivation of the general vector radiative transfer equation (VRTE) describing multiple scattering of light in a volume filled with randomly and sparsely positioned particles of arbitrary size, shape, refractive index, and orientation. That derivation assumed that an observation point was located *inside* the scattering volume. This short note is a natural outgrowth of Ref. 1 in that it explains how the solution of VRTE can be used to calculate the response of a collimated detector of polarized radiation placed *outside* the scattering volume. This problem is important in practice, since scattering objects are often studied with use of external detectors of electromagnetic radiation. Typical examples are remote-sensing observations of the terrestrial atmosphere from earth-orbiting satellites, ground-based telescopic observations of other planets and various astrophysical objects, and bidirectional reflectometry of particle suspensions and particulate surfaces.

The lengthy derivation of Ref. 1 required the introduction of several concepts and specific notation

and the explicit listing of numerous equations. Therefore I will avoid redundancy and save space by assuming that the reader is familiar with Ref. 1 and by using exactly the same terminology and notation.

2. Coherent Field

As in Ref. 1, I consider the scattering of a plane electromagnetic wave $\mathbf{E}^{\text{inc}}(\mathbf{r}) = \mathbf{E}_0^{\text{inc}} \exp(ik_1 \hat{\mathbf{s}} \cdot \mathbf{r})$ by a bounded volume V uniformly filled with independently scattering particles of arbitrary size, shape, refractive index, and orientation. The wave propagates in the direction of the unit vector $\hat{\mathbf{s}}$ and is characterized by the amplitude $\mathbf{E}_0^{\text{inc}}$ and the wave number k_1 . Using the approximations summarized in Section 4 of Ref. 1, let us first address the computation of the coherent field $\mathbf{E}_c^{\text{ex}}(\mathbf{r})$ at an external observation point $\mathbf{r} \notin V$, where “ex” stands for external. The analysis described in Subsection 3.E of Ref. 1 indicates that only forward-scattering particles that lie on the line connecting the source of illumination and the observation point can contribute to the coherent field. Hence, let us consider three possible types of location of the observation point with respect to the scattering volume, as shown in Fig. 1. The line connecting the source of illumination and observation point 1 does not go through the scattering volume, whereas the lines through the source of illumination and observation points 2 and 3 do. However, only in the case of observation point 3 does the scattering volume lie between the source of illumination and the

M. I. Mishchenko (crmim@giss.nasa.gov) is with the NASA Goddard Institute for Space Studies, 2880 Broadway, New York, New York 10025.

Received 11 February 2003; revised manuscript received 14 May 2003.

0003-6935/03/244963-05\$0.00/0

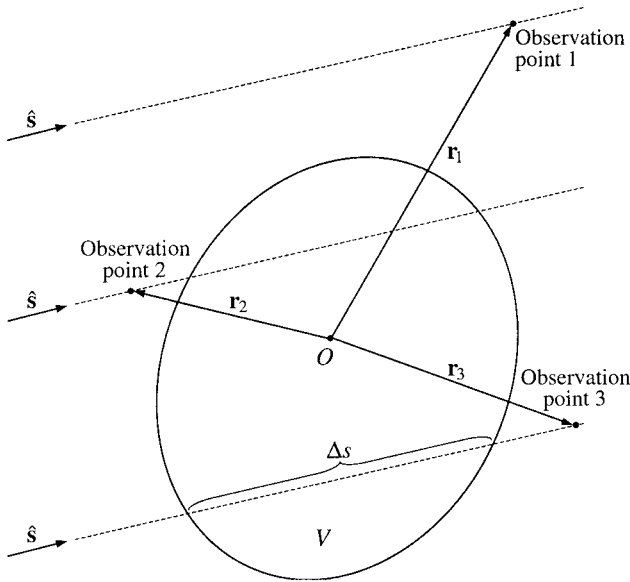


Fig. 1. Coherent field at external observation points.

observation point. Therefore repeating the derivation of Subsection 3.E of Ref. 1 yields

$$\mathbf{E}_c^{\text{ex}}(\mathbf{r}_1) = \mathbf{E}^{\text{inc}}(\mathbf{r}_1), \quad (1)$$

$$\mathbf{E}_c^{\text{ex}}(\mathbf{r}_2) = \mathbf{E}^{\text{inc}}(\mathbf{r}_2), \quad (2)$$

$$\mathbf{E}_c^{\text{ex}}(\mathbf{r}_3) = \exp\left[\frac{i2\pi n_0}{k_1} \Delta s \langle \vec{A}(\hat{\mathbf{s}}, \hat{\mathbf{s}}) \rangle\right] \cdot \mathbf{E}^{\text{inc}}(\mathbf{r}_3), \quad (3)$$

where n_0 is the particle number density, Δs is the length of the light path inside the scattering volume as shown in Fig. 1, and $\langle \vec{A}(\hat{\mathbf{s}}, \hat{\mathbf{s}}) \rangle$ is the ensemble-averaged forward-scattering amplitude matrix per particle. This result can be summarized by the following formula:

$$\mathbf{E}_c^{\text{ex}}(\mathbf{r}) = \begin{cases} \mathbf{E}^{\text{inc}}(\mathbf{r}) & \text{if } \mathbf{r} \text{ is not "shadowed" by } V, \\ \exp\left[\frac{i2\pi n_0}{k_1} \Delta s(\mathbf{r}) \langle \vec{A}(\hat{\mathbf{s}}, \hat{\mathbf{s}}) \rangle\right] \cdot \mathbf{E}^{\text{inc}}(\mathbf{r}) & \text{if } \mathbf{r} \text{ is "shadowed" by } V, \end{cases} \quad (4)$$

where Δs is a function of \mathbf{r} .

By analogy with Subsection 3.F of Ref. 1, Eq. (4) can be rewritten in terms of the Stokes column vector of the external coherent field $\mathbf{I}_c^{\text{ex}}(\mathbf{r})$:

$$\mathbf{I}_c^{\text{ex}}(\mathbf{r}) = \begin{cases} \mathbf{I}^{\text{inc}} & \text{if } \mathbf{r} \text{ is not "shadowed" by } V, \\ \exp[-n_0 \Delta s(\mathbf{r}) \langle \mathbf{K}(\hat{\mathbf{s}}) \rangle] \mathbf{I}^{\text{inc}} & \text{if } \mathbf{r} \text{ is "shadowed" by } V, \end{cases} \quad (5)$$

where \mathbf{I}^{inc} is the Stokes column vector of the incident field and $\langle \mathbf{K}(\hat{\mathbf{s}}) \rangle$ is the ensemble-averaged extinction matrix per particle. The physical interpretation of this formula is very simple: The intensity of the coherent wave is exponentially attenuated and its polarization state changes if and only if the wave travels through the scattering medium.

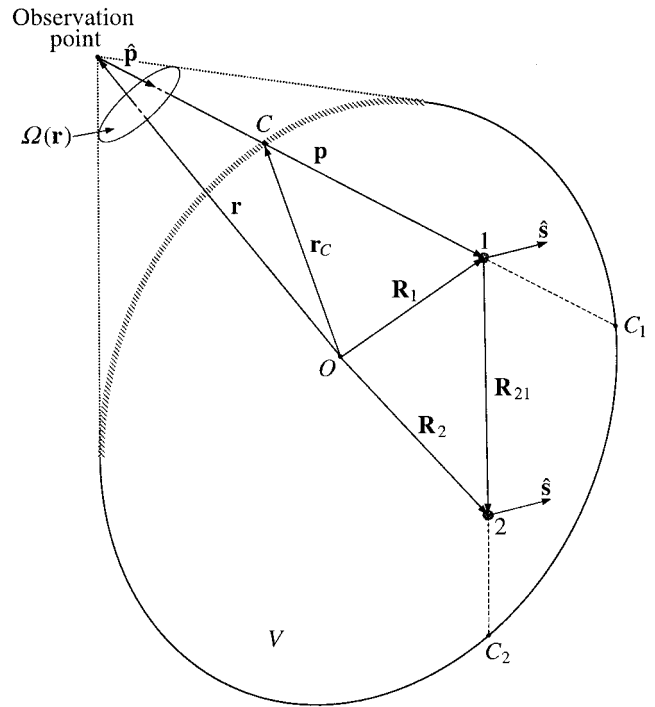


Fig. 2. Coherency dyad at an external observation point.

3. Coherency Dyad

The derivation of the formula for the coherency dyad $\vec{C}^{\text{ex}}(\mathbf{r}) = \langle \mathbf{E}(\mathbf{r}) \otimes \mathbf{E}^*(\mathbf{r}) \rangle$ defined in terms of the total electric field $\mathbf{E}(\mathbf{r})$ at an external observation point $\mathbf{r} \notin V$ is very similar to that for the coherency dyad at an internal point, as described in Subsections 3.G and 3.H of Ref. 1. The only significant difference is that now only a part of the line connecting the observation point and particle 1 (see Fig. 2) lies inside the scattering volume (see Fig. 17 of Ref. 1). Therefore the

final result is as follows:

$$\vec{C}^{\text{ex}}(\mathbf{r}) = \int_{4\pi} d\hat{\mathbf{p}} \vec{\Sigma}^{\text{ex}}(\mathbf{r}, -\hat{\mathbf{p}}), \quad (6)$$

where the vector \mathbf{p} originates at the observation point, $\hat{\mathbf{p}} = \mathbf{p}/p$ is the unit vector in the direction of \mathbf{p} , and the specific coherency dyad $\vec{\Sigma}^{\text{ex}}(\mathbf{r}, -\hat{\mathbf{p}})$ is the sum of the coherent and diffuse parts:

$$\vec{\Sigma}^{\text{ex}}(\mathbf{r}, -\hat{\mathbf{p}}) = \vec{\Sigma}_c^{\text{ex}}(\mathbf{r}, -\hat{\mathbf{p}}) + \vec{\Sigma}_d^{\text{ex}}(\mathbf{r}, -\hat{\mathbf{p}}). \quad (7)$$

The coherent part is given by

$$\vec{\Sigma}_c^{\text{ex}}(\mathbf{r}, -\hat{\mathbf{p}}) = \delta(\hat{\mathbf{p}} + \hat{\mathbf{s}}) \vec{C}_c^{\text{ex}}(\mathbf{r}), \quad (8)$$

where $\delta(\hat{\mathbf{q}})$ is the solid-angle Dirac delta function,

$$\vec{C}_c^{\text{ex}}(\mathbf{r}) = \mathbf{E}_c^{\text{ex}}(\mathbf{r}) \otimes [\mathbf{E}_c^{\text{ex}}(\mathbf{r})]^* \quad (9)$$

is the coherent part of the “external” coherency dyad $\vec{C}^{\text{ex}}(\mathbf{r})$, and the external coherent field $\mathbf{E}_c^{\text{ex}}(\mathbf{r})$ is given by Eq. (4). The diffuse part of the external specific coherency dyad $\vec{\Sigma}_d^{\text{ex}}(\mathbf{r}, -\hat{\mathbf{p}})$ vanishes if $\hat{\mathbf{p}} \notin \Omega(\mathbf{r})$, where $\Omega(\mathbf{r})$ is the solid angle subtended by the scattering volume when it is viewed from the external observation point \mathbf{r} (see Fig. 2). Otherwise it is given by

$$\begin{aligned} \vec{\Sigma}_d^{\text{ex}}(\mathbf{r}, -\hat{\mathbf{p}}) = n_0 \int_C^{C_1} dp \int d\xi_1 \vec{\eta}(-\hat{\mathbf{p}}, p) \cdot \vec{A}_1(-\hat{\mathbf{p}}, \hat{\mathbf{s}}) \cdot \vec{C}_c(\mathbf{r} + \mathbf{p}) \cdot \vec{A}_1^{T*}(-\hat{\mathbf{p}}, \hat{\mathbf{s}}) \\ \cdot \vec{\eta}^{T*}(-\hat{\mathbf{p}}, p) + n_0^2 \int_C^{C_1} dp \int d\xi_1 \int dR_{21} d\hat{\mathbf{R}}_{21} d\xi_2 \vec{\eta}(-\hat{\mathbf{p}}, p) \cdot \vec{A}_1(-\hat{\mathbf{p}}, -\hat{\mathbf{R}}_{21}) \\ \cdot \vec{\eta}(-\hat{\mathbf{R}}_{21}, R_{21}) \cdot \vec{A}_2(-\hat{\mathbf{R}}_{21}, \hat{\mathbf{s}}) \cdot \vec{C}_c(\mathbf{r} + \mathbf{p} + \mathbf{R}_{21}) \cdot \vec{A}_2^{T*}(-\hat{\mathbf{R}}_{21}, \hat{\mathbf{s}}) \\ \cdot \vec{\eta}^{T*}(-\hat{\mathbf{R}}_{21}, R_{21}) \cdot \vec{A}_1^{T*}(-\hat{\mathbf{p}}, -\hat{\mathbf{R}}_{21}) \cdot \vec{\eta}^{T*}(-\hat{\mathbf{p}}, p) + \dots, \quad \hat{\mathbf{p}} \in \Omega(\mathbf{r}), \end{aligned} \quad (10)$$

where \vec{C}_c is the coherent part of the internal coherency dyad, $\vec{\eta}$ is the coherent transmission dyad, and the variable ξ collectively denotes the particle state. The rest of the notation is clear from Fig. 2.

Direct comparison of Eq. (10) with Eq. (113) of Ref. 1 leads us to a fundamental conclusion: The external diffuse specific coherency dyad $\vec{\Sigma}_d^{\text{ex}}(\mathbf{r}, -\hat{\mathbf{p}})$ for a direction $-\hat{\mathbf{p}}$ such that $\hat{\mathbf{p}} \in \Omega(\mathbf{r})$ is equal to the internal diffuse specific coherency dyad at a boundary point C where the line drawn through the observation point in the direction $\hat{\mathbf{p}}$ enters the scattering volume (see Fig. 2). Thus

$$\vec{\Sigma}_d^{\text{ex}}(\mathbf{r}, -\hat{\mathbf{p}}) = \begin{cases} \vec{O} & \text{if } \hat{\mathbf{p}} \notin \Omega(\mathbf{r}), \\ \vec{\Sigma}_d[\mathbf{r}_C(\mathbf{r}, \hat{\mathbf{p}}), -\hat{\mathbf{p}}] & \text{if } \hat{\mathbf{p}} \in \Omega(\mathbf{r}), \end{cases} \quad (11)$$

where \vec{O} is the zero dyad and \mathbf{r}_C is the position vector of the point C (see Fig. 2). Obviously, \mathbf{r}_C is a function of \mathbf{r} and $\hat{\mathbf{p}}$. Equations (6) and (7) then demonstrate that the coherency dyad at the external observation point can be expressed in terms of the internal diffuse specific coherency dyad at those boundary points of the scattering volume that are “visible” from the observation point (the part of the boundary visible from the observation point \mathbf{r} is highlighted in Fig. 2).

4. Specific Intensity Vector

It is straightforward to rewrite Eqs. (7)–(9) and (11) in terms of the specific intensity vector at the external observation point:

$$\vec{I}^{\text{ex}}(\mathbf{r}, -\hat{\mathbf{p}}) = \vec{I}_c^{\text{ex}}(\mathbf{r}, -\hat{\mathbf{p}}) + \vec{I}_d^{\text{ex}}(\mathbf{r}, -\hat{\mathbf{p}}), \quad (12)$$

where

$$\vec{I}_c^{\text{ex}}(\mathbf{r}, -\hat{\mathbf{p}}) = \delta(\hat{\mathbf{p}} + \hat{\mathbf{s}}) \mathbf{I}_c^{\text{ex}}(\mathbf{r}) \quad (13)$$

is the external coherent specific intensity vector,

$$\vec{I}_d^{\text{ex}}(\mathbf{r}, -\hat{\mathbf{p}}) = \begin{cases} \mathbf{0} & \text{if } \hat{\mathbf{p}} \notin \Omega(\mathbf{r}), \\ \vec{I}_d[\mathbf{r}_C(\mathbf{r}, \hat{\mathbf{p}}), -\hat{\mathbf{p}}] & \text{if } \hat{\mathbf{p}} \in \Omega(\mathbf{r}) \end{cases} \quad (14)$$

is the external diffuse specific intensity vector, $\mathbf{I}_c^{\text{ex}}(\mathbf{r})$ is given by Eq. (5), and $\mathbf{0}$ is a four-component zero-column. As was the case with the external diffuse specific coherency dyad, the external diffuse specific intensity vector for a direction $-\hat{\mathbf{p}}$ such that $\hat{\mathbf{p}} \in \Omega(\mathbf{r})$ is equal to the internal diffuse specific intensity vector at that boundary point where the line drawn through the observation point in the direction $\hat{\mathbf{p}}$ enters the scattering volume (Fig. 2). Furthermore, \vec{I}_d^{ex}

$(\mathbf{r}, -\hat{\mathbf{p}})$ vanishes for all directions $-\hat{\mathbf{p}}$ such that $\hat{\mathbf{p}} \notin \Omega(\mathbf{r})$.

5. Discussion

The physical significance of these results follows from the discussion in Section 4 of Ref. 1 and is illustrated in Fig. 3. All four external polarization-sensitive, well-collimated detectors have the same surface area ΔS and the same (small) angular aperture. However, the orientations of the detectors and their positions are different. To emphasize the difference in the orientations of the four detector acceptance solid angles, we denote the latter as $\Delta\Omega_1$, $\Delta\Omega_2$, $\Delta\Omega_3$, and $\Delta\Omega_4$, whereas the position vectors of the respective observation points are denoted as \mathbf{r}_1 , \mathbf{r}_2 , \mathbf{r}_3 , and \mathbf{r}_4 .

Detector 1 faces the incident wave, but its acceptance solid angle $\Delta\Omega_1$ captures no boundary points of the scattering volume. Therefore the polarization signal measured by the first detector per unit time is given by

$$\text{Signal 1} = \Delta S I^{\text{inc}}. \quad (15)$$

Detector 2 is positioned and oriented such that its acceptance solid angle $\Delta\Omega_2$ does not capture the incidence direction, but captures all points of the part of the boundary denoted S_2 . Therefore the polarized signal measured by this detector per unit time is given by

$$\begin{aligned} \text{Signal 2} &= \Delta S \int_{4\pi} d\hat{\mathbf{p}} \vec{I}_d^{\text{ex}}(\mathbf{r}_2, -\hat{\mathbf{p}}) \\ &= \Delta S \int_{\Delta\Omega_2} d\hat{\mathbf{p}} \vec{I}_d[\mathbf{r}_C(\mathbf{r}_2, \hat{\mathbf{p}}), -\hat{\mathbf{p}}], \end{aligned} \quad (16)$$

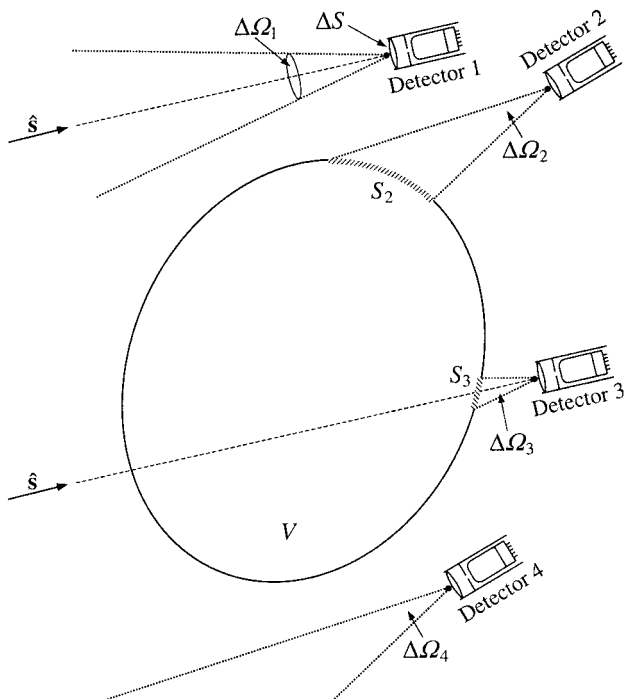


Fig. 3. Polarized signal measured by an external collimated detector depends on the detector position and orientation with respect to the scattering volume.

where, as before, the unit vector $\hat{\mathbf{p}}$ originates at observation point 2 and $\mathbf{r}_C \in V$ is the position vector of the point where the line drawn through the observation point in the direction $\hat{\mathbf{p}}$ crosses the boundary of the scattering volume (see Fig. 2).

The acceptance solid angle of detector 3 captures both the incidence direction and all points of the part of the boundary denoted S_3 . Therefore the polarized signal measured by detector 3 per unit time is

$$\text{Signal 3} = \Delta S \exp[-n_0 \Delta s(\mathbf{r}_3) \langle \mathbf{K}(\hat{\mathbf{s}}) \rangle] I^{\text{inc}} + \Delta S \int_{\Delta\Omega_3} d\hat{\mathbf{p}} \tilde{\mathbf{I}}_d[\mathbf{r}_C(\mathbf{r}_3, \hat{\mathbf{p}}), -\hat{\mathbf{p}}], \quad (17)$$

where, as before, $\Delta s(\mathbf{r}_3)$ is the length of the path traveled by the coherent wave inside the scattering volume before it reaches observation point 3 (see Fig. 1).

Finally, neither the incidence direction nor any boundary point is captured by the acceptance solid angle of detector 4. Therefore this detector measures no signal:

$$\text{Signal 4} = 0. \quad (18)$$

6. First-Order Scattering by a Small Volume Element

In this section we will use the above results to derive the formulas of the so-called first-order-scattering approximation for a small volume element containing a tenuous collection of randomly positioned particles.

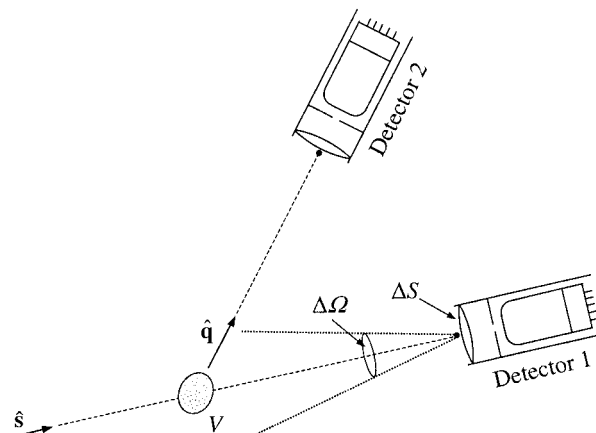


Fig. 4. First-order scattering by a small volume element.

Specifically, let us assume that the number of particles is sufficiently small that

$$|n_0 L \langle \mathbf{K}(\hat{\mathbf{q}}) \rangle_{pq}| \ll 1 \quad \text{and} \quad |n_0 L \langle \mathbf{Z}(\hat{\mathbf{q}}, \hat{\mathbf{q}}') \rangle_{pq}| \ll 1 \quad (19)$$

for $p, q = 1, \dots, 4$ and for any $\hat{\mathbf{q}}$ and $\hat{\mathbf{q}}'$, where L is the largest linear dimension of the volume element and $\langle \mathbf{Z}(\hat{\mathbf{q}}, \hat{\mathbf{q}}') \rangle$ is the ensemble-averaged phase matrix per particle. As a consequence, one may neglect all terms proportional to powers of n_0 higher than the first.

This situation is shown schematically in Fig. 4, where the diameter of the sensitive area of either detector is assumed to be significantly greater than L , and the angular aperture $\Delta\Omega$ of either detector is large enough to encompass the entire scattering volume. We will further assume that the distance r from the volume element to the detectors is much greater than L so that the waves scattered by different particles toward either detector propagate in essentially the same direction, and the distance from the observation point to any particle inside the volume element is approximately the same. Comparison with Fig. 3 shows that the electromagnetic response of detector 1 is described by Eq. (17), whereas that of detector 2 is given by Eq. (16). Let us now recall the integral form of the VRTE,

$$\tilde{\mathbf{I}}_d(Q, \hat{\mathbf{q}}) = n_0 \int_0^Q dq \mathbf{H}(\hat{\mathbf{q}}, Q - q) \langle \mathbf{Z}(\hat{\mathbf{q}}, \hat{\mathbf{s}}) \rangle \mathbf{I}_c(q) + n_0 \int_0^Q dq \int_{4\pi} d\hat{\mathbf{q}}' \mathbf{H}(\hat{\mathbf{q}}, Q - q) \times \langle \mathbf{Z}(\hat{\mathbf{q}}, \hat{\mathbf{q}}') \rangle \tilde{\mathbf{I}}_d(q, \hat{\mathbf{q}}'), \quad (20)$$

where \mathbf{H} is the coherent transmission Stokes matrix and the scattering geometry is shown in Fig. 18 of Ref. 1. We can now use Eqs. (102) and (103) of Ref.

1 to derive that the polarized signal measured by detector 1 per unit time is given by

$$\begin{aligned} \text{Signal 1} = & \Delta S \mathbf{I}^{\text{inc}} - N \langle \mathbf{K}(\hat{\mathbf{s}}) \rangle \mathbf{I}^{\text{inc}} \\ & + \frac{1}{r^2} \Delta S N \langle \mathbf{Z}(\hat{\mathbf{q}}, \hat{\mathbf{s}}) \rangle \mathbf{I}^{\text{inc}}, \end{aligned} \quad (21)$$

whereas that measured by detector 2 per unit time is given by

$$\text{Signal 2} = \frac{1}{r^2} \Delta S N \langle \mathbf{Z}(\hat{\mathbf{q}}, \hat{\mathbf{s}}) \rangle \mathbf{I}^{\text{inc}}, \quad (22)$$

where $N = n_0 V$ is the total number of particles in the volume element.

Equations (21) and (22) are usually used as an *a priori* starting point in the phenomenological derivation of the VRTE (e.g., Ref. 2). The deficiencies of the phenomenological approach are many and have been thoroughly discussed in Refs. 1 and 2. It is, therefore, logical to derive Eqs. (21) and (22) from the self-consistent microphysical radiative transfer theory, which also helps to define the range of applicability of these formulas.

7. Concluding Remarks

I have shown in this paper that if VRTE has been solved and, as a consequence, the diffuse specific intensity vector is known at all points of the scattering

volume, then Eqs. (12)–(18) can be used to calculate the polarization response of an external collimated detector arbitrarily oriented and positioned with respect to V . I have also used Eqs. (16) and (17) along with the integral form of the VRTE to derive the formulas of the first-order-scattering approximation for a small volume element observed from a distance much greater than the largest linear dimension of the volume element. Although heuristic analogues of these results have been widely used in the framework of the phenomenological radiative transfer theory, it was important to demonstrate that Eqs. (12)–(18), (21), and (22) can be consistently derived using the microphysical approach based on methods of statistical electromagnetics.

I thank Yuri Barabanenkov, Anatoli Borovoi, Joop Hovenier, and Cornelis van der Mee for many fruitful discussions and Nadia Zakharova for help with graphics. This research was funded by the NASA Radiation Sciences Program managed by Donald Anderson.

References

1. M. I. Mishchenko, "Vector radiative transfer equation for arbitrarily shaped and arbitrarily oriented particles: a microphysical derivation from statistical electromagnetics," *Appl. Opt.* **41**, 7114–7134 (2002).
2. L. A. Apresyan and Yu. A. Kravtsov, *Radiation Transfer: Statistical and Wave Aspects* (Gordon and Breach, Basel, Switzerland, 1996).